Integrating optics and micro-mechanics in a single substrate: a step toward monolithic integration in fused silica.

Yves Bellouard

CAT/CIE, Rensselaer Polytechnic Institute, CII 8011, 110, 8th Street, Troy, NY, USA.
Present address: Micro- & Nano- Scale Eng., Mechanical Eng., Eindhoven University of Technology, PO Box 513, 5600 MB Eindhoven, The Netherlands.
y.bellouard@tue.nl

Ali A. Said, Philippe Bado

Translume Inc., 655, Phoenix Drive, Ann Arbor, MI, USA.

Abstract: We present a novel optical sensor concept that merges integrated optics and micro-mechanics in a monolithic substrate. This concept pushes microsystems integration and defines a new class of monolithic optical microsystems where only optical signals are processed. As an illustration, we present a high-precision, monolithic, glass-based, micro-displacement sensor. Our displacement sensor is made out of a single piece of glass through a two-step process based on femtosecond laser illumination followed by chemical etching.

©2005 Optical Society of America

OCIS codes: (230.1150) All-optical devices; (230.7370) Waveguides; (220.4880) Optomechanics; (220.4000) Microstructure fabrication; (130.3120) Integrated optics devices; (120.3930) Metrological instrumentation; (320.7130) Ultrafast processes in condensed matter, including semiconductors.

References and Links

1. Y. Bellouard, PhD dissertation (no 2308), Ecole Polytechnique Fédérale de Lausanne, 2000.
2. K. M. Davis, K. Miura, N. Sugimoto, K. Hirao, "Writing waveguides in glass with a femtosecond laser," Opt. Lett. **21**, 1729-1731 (1996).
3. A. Marcinkevičius, S. Juodkazis, M. Watanabe, M. Miwa, S. Matsuo, H. Misawa, J. Nishii, "Femtosecond laser-assisted three-dimensional microfabrication in silica," Opt. Lett. **26**, 277-279 (2001).
4. P. Bado, A. A. Said, M. Dugan, T. Sosnowski, S. Wright, "Dramatic Improvements in Waveguide Manufacturing with Femtosecond Lasers" in NFOEC, Dallas (TX), Sept. 2002.
5. Y. Bellouard, A. Said, M. Dugan, P. Bado, "Fabrication of High-Aspect Ratio, Micro-Fluidic Channels and Tunnels using Femtosecond Laser Pulses and Chemical Etching," Opt. Express **12**, 2120-2129 (2004), http://www.opticsexpress.org/abstract.cfm?URI=OPEX-12-10-2120.
6. P. Bado, A. Said, M. Dugan, "Manufacturing of high quality integrated optical components by laser direct-write," in ICALEO, Jacksonville (FL), Oct. 2003.
7. S. Ungar, *Fiber Optics, Theory and Applications*, (John Wiley & Sons, NY, ISBN 0 417 92758 9, 1990).
8. R.V. Jones, Parallel and rectilinear spring movements, J. Sci. Instrum. **28**, 38-41 (1951).
9. S. T. Smith, D.G. Chetwynd, Foundations of Ultraprecision Mechanism Design, ed. Gordon & Breach Publishers.
10. J.M. Paros, L. Weisborg, Machine Design **27**, 151-156 (1965).
11. S. Henein, "Conception des guidages flexibles," Press Polytechniques et Universitaires Romandes, 2001.
12. H. Scholze, *Glass: Nature, Structure and Properties*, (Springer-Verlag publishers, 1990).

1. Introduction: monolithic integration at the micro-scale

As miniaturization progresses, microsystems integrate a larger number of functionalities in a small volume. This integration poses numerous challenges, from the conceptual stage to the manufacturing. We propose an approach based on multifunction integration in *monolithic* substrates – in other words we turn a single substrate into a system by locally tailoring its properties.

#7625 - $15.00 USD Received 1 June 2005; revised 16 August 2005; accepted 16 August 2005

The principle of localized “functionalization” is well known in life sciences. For instance, in proteomics and genomics, molecules are partially modified in order to give them a capability to “combine” with another molecule. In biodetection, surfaces are functionalized by adding a specific receptor that will match a corresponding biomarker.

In our case, functionalization is understood in a broader sense: it means any *system-level* function that is added through controlled and localized material modifications, with the intent that the material responds to a given stimulus in a specific and controlled manner. The latter implies that modifications are not done randomly or globally but according to a particular scheme determined by the desired system function.

Monolithic integration has multiple advantages – straightforward assembly, higher accuracy, increased reliability, simpler packaging, miniaturization, etc. – that derive from the fact that we are dealing with a single piece of material.

This monolithic integration through localized functionalization concept was proposed by one of the authors to integrate passive and active parts in a single piece of Shape Memory materials [1]. Here, we extend it to system integration in fused silica substrates using femtosecond laser and chemical processing.

Recent progresses in the processing of fused silica with femtosecond lasers have opened new opportunities for microsystems design: Davis *et al.* [2] demonstrated waveguides writing; and Marcinkevičius *et al.* [3] showed the effect of chemical etching on femtosecond laser irradiated parts. Building on these foundations, we introduced the concept of “painting” [4], which allows for the fabrication of arbitrary shaped optical waveguides. We also demonstrated the fabrication of micro-fluidic channels of arbitrary sizes ([5]).

In this paper, we further push the concept of monolithic integration through localized functionalization by combining waveguide writing and channel etching in fused silica. We merge micro-mechanical and optical functions in a common substrate. As an illustration, we present a displacement micro-sensor made of a single piece of fused silica using the combination of femtosecond laser exposure and chemical etching.

2. Displacement micro-sensor design and fabrication

2.1 Sensor concept overview

The “all-optical” sensor is shown in Fig. 1. A force applied to the sensor tip induces a linear motion of the mobile platform. The sensor has two key elements: a flexure-based micro-mechanism that accurately guides the motion of the platform along one axis, and a waveguide-based element that senses a displacement. This displacement-sensing element consists of an array of optical waveguides embedded in the moving platform and two waveguide segments embedded in the stationary frame. We call this detection system “Integrated Linear Encoder” (ILE).

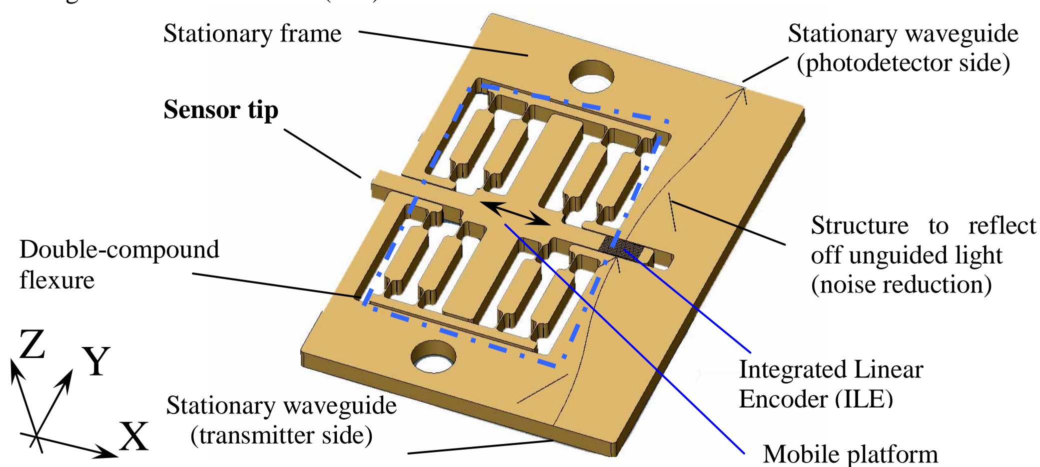

Fig. 1. Computer Assisted Drawing view of the full sensing device.

#7625 - $15.00 USD
Received 1 June 2005; revised 16 August 2005; accepted 16 August 2005
(C) 2005 OSA

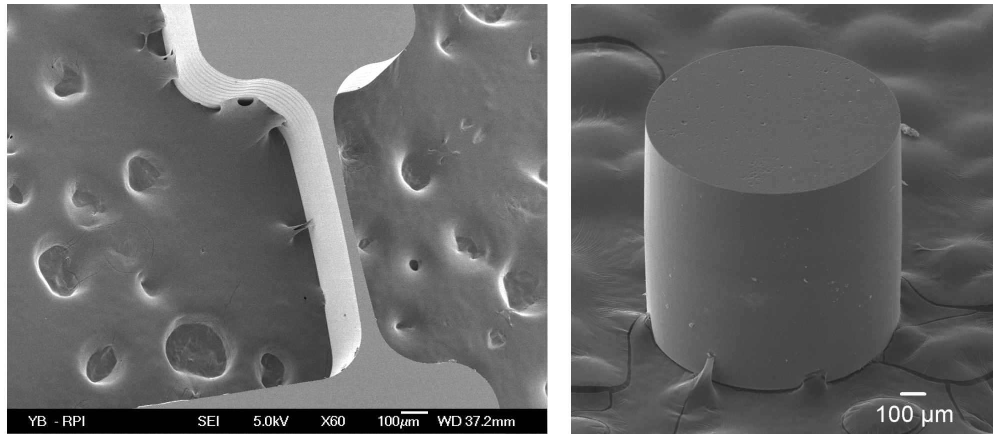

Fig. 2. A micro-hinge (left) and a cylinder (right) manufactured using the hybrid femtosecond / chemical etching process.

2.2 Micro-fabrication process

The sensor is machined out of a fused silica substrate using a two-step fabrication process based on femtosecond laser irradiation and chemical etching [3,5]. Waveguides and shape contours are introduced by illuminating a predefined pattern with a femtosecond laser, whose power is sufficiently low to avoid ablation. Waveguide manufacturing parameters have been described in detail elsewhere [4,6], briefly the laser used generated 100-fs (800nm) pulses at 250 kHz. The laser was focused with a 50x objective. The scanning speed varies from 0.05mm/sec to 2mm/sec. The laser pulse energy was typically 0.3 µJ for waveguide manufacturing and 0.8 µJ for etching. For the specific range of power used, the laser affects two of the fused silica properties: it increases locally its refractive index [2] and its HF chemical etching selectivity [3,5]. Noticeably, since the laser-matter interaction is essentially non-linear and mostly driven by multi-photon absorption, the material is only affected at the focal point once a power threshold is reached. As a consequence and since fused silica is transparent at the laser wavelength considered (800 nm), affected zones can be introduced below the glass surface.

After laser exposure, the substrate is etched in a low concentration HF bath. The measured etching rate is on the order of a few microns per min in the exposed region as opposed to a few microns per hour for the raw (i.e. unexposed) material. The highly anisotropic etching, resulting from the laser exposure, makes the fabrication of high-aspect ratio structures possible using appropriate pattern generation methods. Our laser patterns are made of multiple linear passes stacked in three dimensions. Further details can be found in [5].

Fig. 2 shows SEM pictures of a notch hinge (left) and a cylinder (right) cut out of a 0.5 and 1 mm-thick glass respectively. A key aspect of our method is that the various structural, mechanical and optical elements are all introduced with the same laser workstation in a continuous manufacturing process. Specifically, there is no *need for repositioning of the work piece*. Consequently, this manufacturing technology is intrinsically very accurate: the positioning accuracy only depends on the performance of the motorized stages used to move the specimen under the laser beam.

2.3 "Integrated Linear Encoder" (ILE)

We used the variation of signal intensity induced by lateral misalignment between identical waveguides as the basic principle for the mobile platform displacement. In practice, a waveguide segment is incorporated in the mobile platform so that, at rest it is aligned with two stationary waveguides used as transmitting and receiving waveguides for the ILE signals.

#7625 - $15.00 USD Received 1 June 2005; revised 16 August 2005; accepted 16 August 2005
(C) 2005 OSA

Using a single waveguide segment in the moving platform would limit the sensing range to approximately the width of the mode-field diameter (MFD). To extend the displacement sensing range, the platform contains an array of parallel waveguides. When a waveguide segment of the movable platform is aligned with the input and output stationary waveguides (parts Fig. 3(a) and Fig. 3(c)), the intensity of the transmitted signal is maximized.

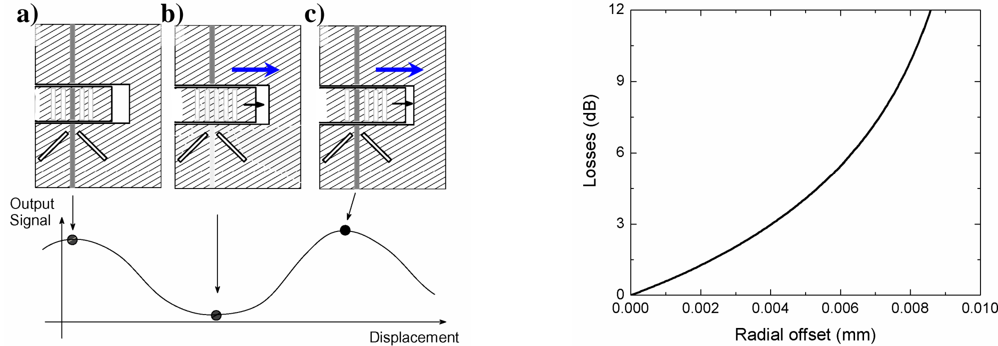

Fig. 3. Left: "Waveguides-based linear encoders principles"– Right: Losses due to radial offset between two waveguides with 10-microns core diameter.

Conversely, when the waveguides are misaligned (Fig. 3(b)), the light is no longer guided through the platform (it is only guided in the input segment), which results in a severe loss of transmitted signal. The range of motion sensing can be extended indefinitely with this approach.

Using a simple model based on geometrical considerations (neglecting the Fresnel losses at the interfaces) and considering two waveguides laterally misaligned, the corresponding losses can be approximated by (expressed in dB) [7]:

$$L_{lat} = -10\log\left\{\frac{2}{\pi}\left[\cos^{-1}\left(\frac{\delta}{D}\right)-\frac{\delta}{D}\sqrt{1-\left(\frac{\delta}{D}\right)^{2}}\right]\right\} \quad (1)$$

Where, in the case of a single mode waveguide, D is the waveguide mode-field diameter (MFD) and δ the lateral misalignment. Losses are shown in Fig. 3 (right). This simple power loss estimation illustrates the device sensitivity to misalignment: a few microns motion results in sharp power losses. We exploit this property to sense the displacement of the sensor tip. Note that equation 1 does not account for the additional optical losses that are present in our device (gap between the moveable platform and the static frame, multimode propagation, waveguide size mismatch, etc.)

Eq. (1) does not account for potential coupling effects between parallel waveguides. A more accurate model, a full wave propagation analysis for the integrated linear encoder is presented below.

Further, the ILE operates properly only if a sub-micron linear guiding accuracy is maintained while the sensor tip moves. The guiding function is realized by integrating a double-compound flexure into the system. The kinematics principle is described in the next section.

2.4 Kinematics

The kinematics model is based on two identical four-bar mechanisms serially connected, as shown in Fig. 4(c). This kinematics design is well known in precision engineering (see for instance [8,9]). In a parallelogram four-bar mechanism (Fig. 4(a)), the mobile platform moves along an arc relative to the ground (i.e. the stationary part). To first approximation, when the arc radius is large (i.e. long bars and small motion) the mobile element trajectory is quasi-linear. In our case, we have the additional requirement that a constant gap must be maintained

#7625 - $15.00 USD Received 1 June 2005; revised 16 August 2005; accepted 16 August 2005
(C) 2005 OSA

between the mobile platform and the fixed frame. This can be achieved by serially connecting two identical four-bar parallelogram mechanisms as shown in Fig. 4(b).

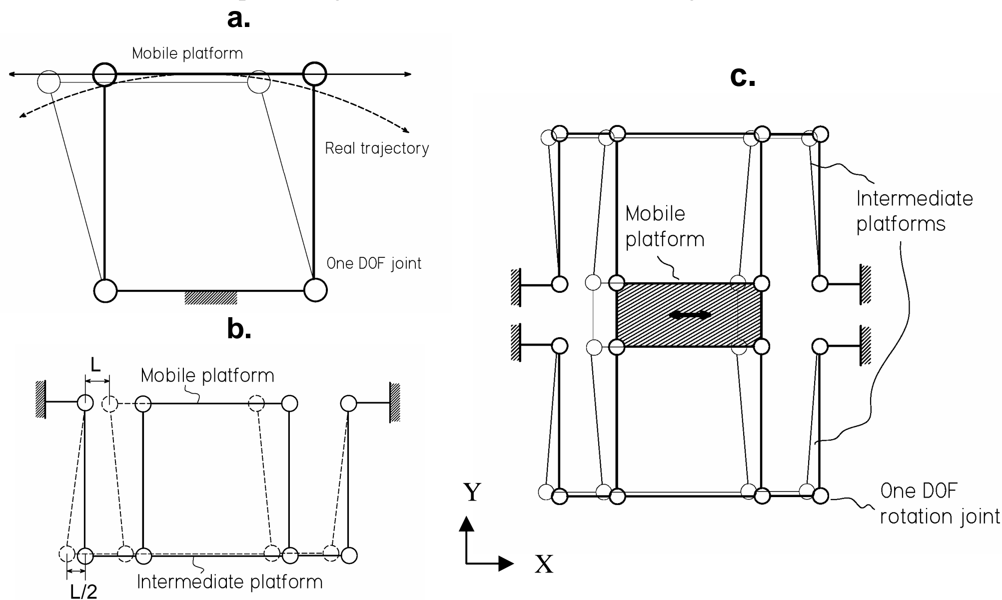

Fig. 4. Sensor kinematics: the circle represents ideal mechanical joints with one degree of freedom (rotation in the plane). Figure a) is a parallelogram four-bars mechanism, b) represents a single compound design and c) a double-compound design

This configuration introduces a so-called "internal mobility" (i.e. internal motion that exists even if input and output of the mechanism are blocked). In the case shown in Fig. 4(b), the intermediary platform can move even if the mobile platform is blocked. This internal mobility is not controlled and can be activated by external disturbances (i.e. vibrations, external loads, acceleration¸ etc.) that can lead to motion interference with the mobile platform. A practical way to remove this undesirable internal mobility is to use a double-compound rectilinear kinematics structure as shown in Fig. 4(c) [8,9]. This strategy offers the additional advantage that it is self-compensated for thermal-expansion.

Fig. 4 shows idealized rotational joints. In microengineering, due to scale and precision requirements, such a mechanical design is difficult to implement with multiple parts. Rather, a monolithic, flexure-type design is preferred. The principle is to replace traditional (i.e. multipart joints) by elastic hinges to realize the same kinematics. In our case, we use a notch-hinge to emulate the behavior of a rotational joint [10].

3. Sensor modeling

We now explore in more details the sensor design. In a first section we present the ILE modeling from an optical beam propagation perspective. Actual physical characteristics and dimensions are taken into account to reflect as much as possible the real system. In a second section, we further detail the actual double-compound flexures and present FEM simulation of their mechanical behavior.

3.1 Waveguide modeling

The ILE consists of a fixed 30μm pitch waveguide array spanning the 1-mm end section of the movable platform (Fig. 1 and Fig. 3 left). By design, a transmitting and a receiving waveguide in the stationary section of the flexure mount are in direct axial alignment with one of the array waveguides when the stage is unloaded and at rest.

#7625 - $15.00 USD Received 1 June 2005; revised 16 August 2005; accepted 16 August 2005
(C) 2005 OSA

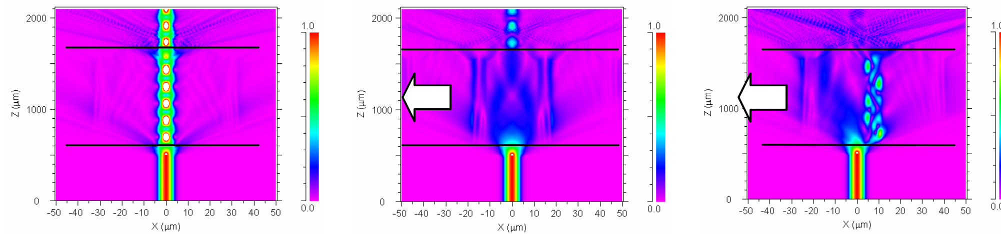

Fig. 5. Wave propagation in the ILE for various configurations as the array is moved from the right to the left. The horizontal line indicates the free space gaps (Movie: 858kb).

The optical signal crosses two identical free space gaps (schematically represented by straight lines in Fig. 5) – one located between the output of the transmitting waveguide and the input of the movable array waveguides; and a second located between the output of the array waveguides and the input of the receiving waveguide. These gaps consist of a 30-µm air region sandwiched between two 20-µm glass region where the light is unguided.

The waveguides are 8µm wide with an index difference (core – cladding) of ~5.25e-3. They are highly multimode at the test wavelength of 670 nm. The refractive index value used for the waveguide modeling was previously measured using a commercial RNF tool [4,6].

Light propagation through the structure is simulated using the finite difference method. The fundamental mode at 670 nm is launched into the input waveguide. After the propagation is completed the output waveguide power is recorded, the array is displaced from the stationary waveguides by 0.6µm, and the propagation is restarted. This is repeated through a couple of periods of the array.

Beam expansion of the fundamental mode across the first gap results in a finite overlap with higher order modes at the input of the corresponding array waveguide even when the waveguides are perfectly aligned. From there on the optical signal propagates in a multimode fashion as can be seen in the simulation video (Fig. 5). Despite the multimode nature, the roll-off of a single waveguide transmission with displacement is monotonic and can be scaled with distance (Fig. 10 measurement vs. simulation plot). This type of signal response is maintained as long as the array pitch is large enough to prevent coupling between the parallel waveguides. Fig. 10 also shows a secondary peak at half-pitch displacements. This signal is from free-space propagation across the 1-mm wide moveable platform.

3.2 Flexure modeling

Keeping in mind the desired kinematics, we model the double compound flexure, first by introducing a simple analytical model to optimize the design parameters, and second by Finite Element Modeling.

Analytical model

We first consider a parallel four-bar mechanism and assume that every hinge is equally loaded (i.e. the point where force is applied lies on an axis parallel to the motion axis and located at equal distance from two adjacent hinges). We also assume small deformations and a pure elastic material behavior. For small angles, the stiffness of the four bar structure can be reasonably approximated by [11]:

$$K_x \approx \frac{8Ebt^{2.5}}{9\pi l^2 \sqrt{r}} \tag{2}$$

Where E is the Young's modulus, t the notch hinge thickness, b the plate thickness (along the Z axis), l the distance from the notch hinge center to the next notch hinge center distributed along the Y-axis and r the notch hinge radius.

Since the complete flexure is made of two four-bars connected in serial forming a first element connected in parallel to a symmetric element, the overall stiffness in the motion direction for the double compound is the same as the single stage one (Fig. 4).

#7625 - $15.00 USD Received 1 June 2005; revised 16 August 2005; accepted 16 August 2005
(C) 2005 OSA

The maximum angular excursion of simple notch hinges can be estimated by [11]:

$$\alpha_M \approx \frac{3\pi\sigma_L\sqrt{r}}{4E\sqrt{t}} \tag{3}$$

Where r is the notch hinge radius, t the hinge thickness along the x direction, E the Young's modulus and σ_L the elastic limit. Considering a given elastic limit σ_L, the range of motion Δy for this mechanism is:

$$\Delta y = \frac{3\pi L\sigma_L\sqrt{r}}{2E\sqrt{t}} \tag{4}$$

Where l is the distance between two notch hinge centers along the Y direction and E the Young's modulus. This result is simply twice the motion of a single stage mechanism (Fig. 4(a)). The following dimensions with corresponding stiffness and range motion values were chosen based on this simple analytical model.

Table 1. Main design parameters

σ_L (MPa)	L (mm)	t (μm)	r (mm)	b (mm)	E (GPa)	Poisson ratio
300	4.7	50	7	1	75	0.17

The analytical model predicts that, for stiffness equals to 0.200 N/mm, a force of 200 mN is required to reach full excursion. The elastic limit σ_L of fused silica is often listed at 50 MPa. It is known that this value depends on the presence or absence of surface flaws. Processes that eliminate these flaws, such as HF etching, can increase the elastic limit by several orders of magnitude [12] As a result, and although this may be counterintuitive, fused silica is an excellent material for micro-mechanical applications. For this work we used an elastic limit of 300 MPa, as shown in Table 1. Experimentally we found this value to be conservative.

Finite Element Modeling - Mechanical structure modeling

To refine and optimize the hinge shape, a finite element analysis was conducted. First a static analysis was conducted as illustrated in Fig. 6. For this simulation, the force applied on the structure along the X-axis is the required force predicted by the analytical model to get the full excursion. Good agreement between analytical and FEA model is found. From the FEA, the force to get the full excursion is about 400 mN and the maximum stress is 240 MPa, as opposed to 200mN and 300 MPa as predicted by the analytical model.

A dynamic study was also conducted. The vibration modes are shown in Fig. 7. The three first modes are inplane vibration (frequencies below 1.5 kHz). The next ones are related to out-of-plane vibrations and are found at much higher frequencies (3.2 to 9.5 kHz).

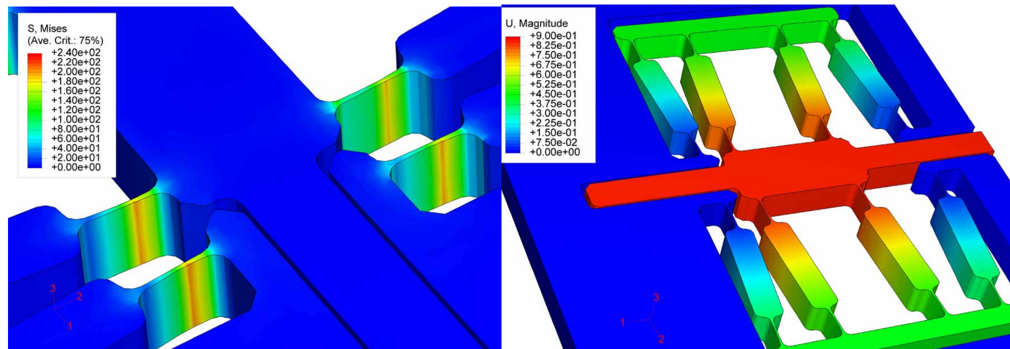

Fig. 6. FEM analysis – Stress distribution in four hinges (left) and displacement distribution of the entire structure (right).

#7625 - $15.00 USD
Received 1 June 2005; revised 16 August 2005; accepted 16 August 2005
(C) 2005 OSA

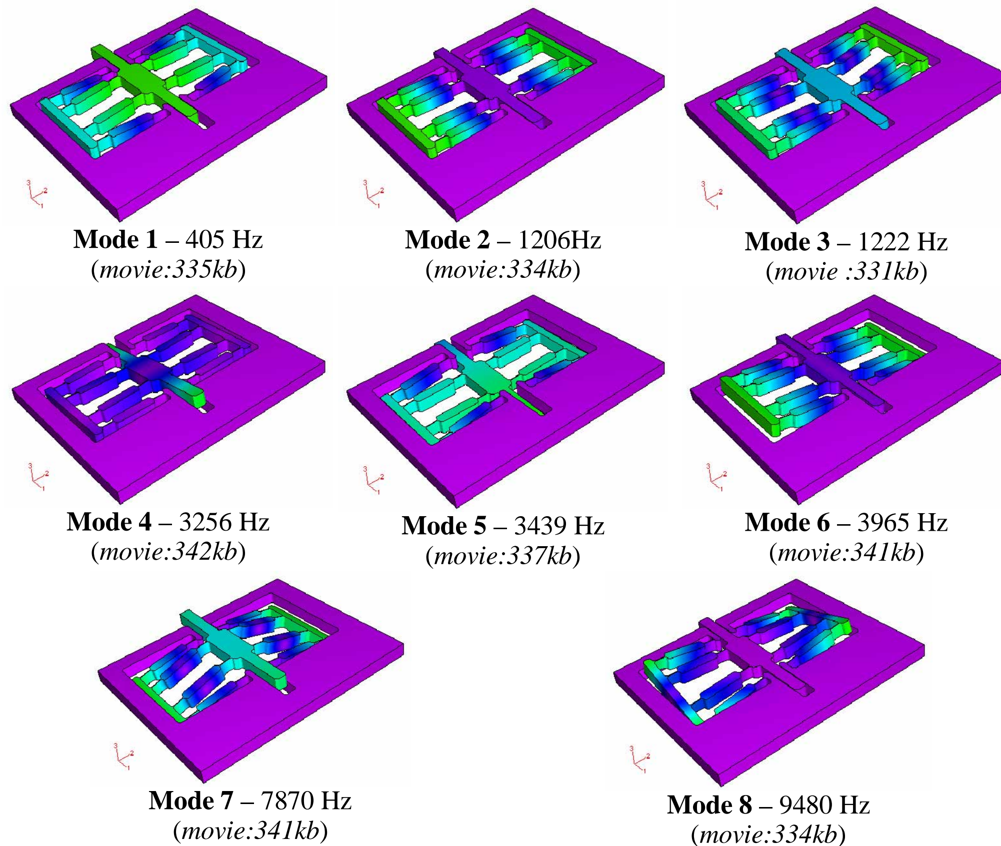

Fig. 7. Flexure vibration mode analysis.

These simulation results show a strong decoupling between the natural vibration mode and the higher order ones. They also show the relatively average dynamic performance of the double compound rectilinear mechanisms since the intermediate members of the symmetrical compensated rectilinear stages can be excited at relatively low frequencies.

4. Experimental setup

A sketch and a partial view of the experimental setup are shown in Fig. 8. The sensor characterization was performed with a free-space optics setup. A mechanical finger is used to apply a displacement on the force sensor tip. The finger is stiff and is attached to a sub-micron accuracy piezo-actuated positioning stage whose stiffness is several orders of magnitude higher than that of the sensor. The finger position is measured using a triangulation measurement system made of a laser beam, a mirror and a position-sensing device. This measurement system has a 50 nm resolution. As the finger applied a force on the sensor tip, the flexure is deformed and the waveguides embedded in the mobile platform moved laterally relative to the stationary waveguide pair. A 670-nm laser diode is used as the light source and is injected into the stationary waveguide. At this wavelength the waveguides are multi-mode. The light intensity transmitted through the sensor is measured by a photodetector. Acquired signals (transmitted intensity, finger position) are further processed.

The fabricated micro-sensor is shown in Fig. 9: the left picture shows an optical microscope view of half of the flexure; the middle and left pictures are close views of the ILE. Waveguides are 8 microns wide and are placed at 100 microns below the surface. There is a total of nine waveguides on the movable platform. The laser-writing took approximately 24 hours. This duration can be significantly reduced by optimizing the contour parameters and the scanning speed.

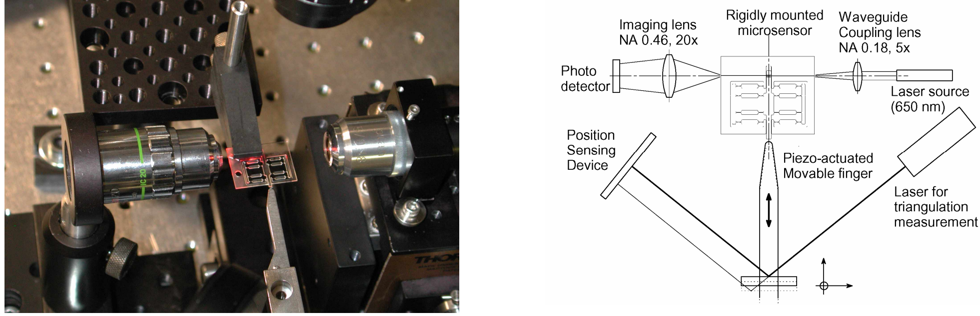

Fig. 8. Experimental setup: (left) Partial view and (right) sketch.

In Fig. 9, the movie linked to the left picture illustrates the glass flexure displacement while the movie linked to the right picture shows how light is sequentially guided and then unguided as the mobile platform moves. Scattering is clearly visible at the interface between the mobile platform and the stationary waveguide.

The light intensity transmitted through the sensor is measured as a function of the finger displacement measured using a laser triangulation technique and crosschecked with an inductive sensor. The acquired signal is recorded and compared with simulation results. The measurement resolution along the X-axis is found to be 50 nm.

The experimental results (shown in Fig. 10) closely resemble the simulated results in section 3.1. The predicted intermediate peak is clearly visible in the experimental curve. We also notice some peak intensity variation for the largest peaks. This variation is typically within +/- 15 % from waveguide to waveguide. These intensity fluctuations may arise from local changes in wall roughness (typ. 300 nm). Inserting an index-matching liquid in the gaps tends to uniform the peak intensity levels.

The first resonant frequency was measured on a prototype having hinges of about 42 +/- 2 um microns as measured under an optical microscope. The measurement was done by imposing a sinusoidal mechanical vibration on the piezo-actuator that drives the moving finger main axis. We found the resonant frequency at 209 Hz. For this hinge thickness, the FEM simulation gives a first mode resonant frequency at 206 Hz showing a good agreement with the experimental results. Using the ILE signal, we know the microstage position with a resolution equal or better than 50–nm. (This positioning accuracy is presently limited by our experimental setup and not by the microstage itself).

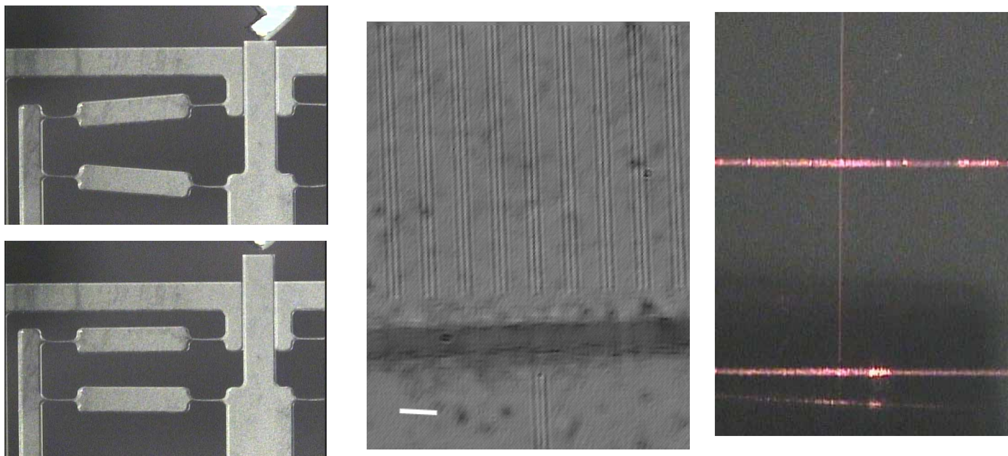

Fig. 9. (left) Sensor prototype: optical microscope view (*movie: 500kb*) / (middle) close-view of the ILE. The scale bar is 30 µm. / (right) waveguide turns on and off (*movie: 748kb*)

#7625 - $15.00 USD Received 1 June 2005; revised 16 August 2005; accepted 16 August 2005
(C) 2005 OSA

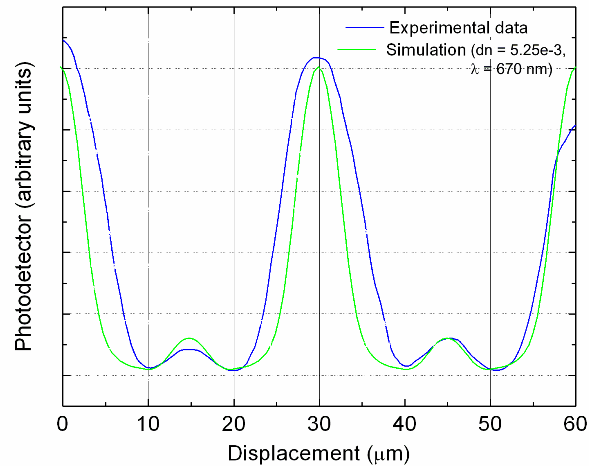

Fig. 10. Experimental results (upper curve) compared with simulation results (lower curve). The figure shows the intensity seen for the last three waveguides (going from left to right). The lowest intensity peaks (on the right) corresponds to the last waveguide.

5. Conclusion

We have demonstrated the integration of micro-mechanical elements and optical waveguides in a monolithic fused silica platform. The waveguides are used to probe the displacement of a moving platform whose motion is precisely guided by a double-compound flexure kinematics.

Although, this paper is mainly focused on a specific device, the concept illustrated here is applicable to a variety of sensors where optical waves are used as the signal source and information carrier.

This approach is particularly useful for sensing in severe electromagnetic or other types of harsh-environment. Noticeably, using fiber optics to get signals in and out of the sensor, the sensor head, i.e. the part physically in contact with its environment, can be put at an arbitrarily long distance from the signal processing element that may contain environment sensitive components like laser diodes and photo detectors

Improvements to the ILE can be realized by incorporating smaller waveguides and/or increasing the number of signal channels. Using multiple transmitting and receiving waveguide pairs sampling the array at different positions would significantly increase displacement detection sensitivity and uniformity. The rate of signal roll-off from exact alignment with any one-array waveguide is determined by mode size and shape approximating a linear response over only a fraction of the displacement. A series of waveguide arrays consisting of different size waveguides between the arrays yet size matched to the corresponding input / output waveguide would allow for a sensitivity scale. The constraint of a minimal waveguide separation within any one array to prevent cross coupling will impose a low signal region around multiple half-pitch displacements. A high sensitivity and high signal level response can be obtained for a single array configuration by sampling the array at a series of fixed offsets. For example, a direction sensitive, quadrature scheme can be realized using a 1 X 4 splitter of the input signal relayed to different positions of the array and aligned at ¼ pitch offsets. Signal threshold will determine which of the 4 receiving waveguides to monitor. With the appropriate choice of waveguides geometry determining mode shape and size, a high and uniform SNR can be maintained for the full range of displacements.

#7625 - $15.00 USD Received 1 June 2005; revised 16 August 2005; accepted 16 August 2005
(C) 2005 OSA